# THE CLUSTER SPATIO-TEMPORAL ANALYSIS OF FIELD FLUCTUATIONS (STAFF) EXPERIMENT

N. CORNILLEAU-WEHRLIN, P. CHAUVEAU, S. LOUIS, A. MEYER, J. M. NAPPA, S. PERRAUT, L. REZEAU, P. ROBERT, A. ROUX and C. DE VILLEDARY *CETP/UVSQ, Vélizy, France* 

Y. DE CONCHY, L. FRIEL, C. C. HARVEY, D. HUBERT, C. LACOMBE, R. MANNING and F. WOUTERS Observatoire de Paris, Meudon, France

F. LEFEUVRE, M. PARROT, J. L. PINÇON and B. POIRIER LPCE/CNRS, Orléans, France

W. KOFMAN CEPHAG, Grenoble, France

PH. LOUARN

Observatoire Midi-Pyrénées, Toulouse, France

AND THE STAFF INVESTIGATOR TEAM

**Abstract.** The Spatio-Temporal Analysis of Field Fluctuations (STAFF) experiment is one of five experiments which together comprise the Wave Experiment Consortium (WEC). STAFF consists of a three-axis search coil magnetometer to measure magnetic fluctuations at frequencies up to 4 kHz, and a spectrum analyser to calculate in near-real time aboard the spacecraft, the complete auto- and cross-spectral matrices using the three magnetic and two electric components of the electromagnetic field. The magnetic waveform at frequencies below either 10 Hz or 180 Hz is also transmitted. The sensitivity of the search coil is adapted to the phenomena theo be studied: the values  $3 \times 10^{-3}$  nT Hz<sup>-1/2</sup> and  $3 \times 10^{-5}$  nT Hz<sup>-1/2</sup> are achieved respectively at 1 Hz and 100 Hz. The dynamic range of the STAFF instruments is about 96 dB in both waveform and spectral power, so as to allow the study of waves near plasma boundaries. Scientific objectives of the STAFF investigations, particularly those requiring four point measurements, are discussed. Methods by which the wave data will be characterised are described with emphasis on those specific to four-point measurements, including the use of the Field Energy Distribution function.

## 1. Introduction

The Cluster mission has been designed to study the thin layers of the interaction regions between the solar wind and the Earth's magnetosphere. The very existence of these regions, with their different plasma bulk properties, is largely due to wave-particle interactions which, in a collisionless plasma, provide the only means of modifying the bulk properties of plasma crossing the frontier. Within these regions, waves again provide the only effective coupling between particles of the same and of different species, and give rise to anomalous transport effects; the basic physics of these regions requires a comprehension of understanding of the

wave-particle interactions present. Thus it is important to characterise the waves and turbulence: this is the objective of the Cluster STAFF measurements. Four point measurements will allow, for the first time, a clear separation of spatial and temporal effects. A major consideration for wave observations in a fast-flowing medium is the Doppler effect. Waveform data from four spacecraft in a tetrahedral configuration allow correction for this effect when the wavelength is comparable with the inter-spacecraft separation. On the other hand, when the wavelength is small compared to the inter-spacecraft separation, the determination of the wave normals on the four separate spacecraft may yield information about the source location. To understand turbulence it is important to measure over a frequency range wide enough to determine any cut-off frequency; instrumentation has sometimes been inadequate for this purpose on earlier missions. Earlier missions have been even less adapted to investigate spatial wavenumber spectra. Furthermore, some geophysically important regions have been rather neglected: for example, the cusp has been visited only by the HEOS spacecraft.

In the next section of this paper, the principle scientific objectives are discussed. Methods by which the wave data will be characterised are described in Section 3, with emphasis on those specific to four-point measurements.

This is followed by a technical description of the STAFF experiment, including the various in-flight modes of operation of the instrument. The experiment has identical instruments on each of the four Cluster spacecraft. Each instrument comprises a three-axis search coil magnetometer to measure the magnetic fluctuations up to 4 kHz, and a spectrum analyser to calculate in near-real time the 5 × 5 cross-spectral matrix formed from the three magnetic and two electric field components, at 27 frequencies, provided by Electric Field and Wave (EFW) experiment, of the electromagnetic field. The vector magnetic field waveform is also transmitted, in a frequency band extending to either 10 Hz or 180 Hz, selectable by telecommand. STAFF is one of the five wave instruments aboard Cluster which form the Wave Experiment consortium (WEC, see Pedersen *et al.*, this issue).

## 2. Scientific Objectives

In this section we present areas where we anticipate that the STAFF experiment will make a significant contribution to our current understanding of the plasma physics of Earth's environment. Telemetry and ground station limitations do not allow full 24 hr per day data coverage along the whole Cluster orbit. Thus, in what follows, we mainly discuss those regions which are primary objectives of the Cluster mission and for which data acquisition is a priority. The papers cited are mostly recent work, or reviews in which references to earlier pioneer work can be found.

#### 2.1. SOLAR WIND AND UPSTREAM WAVES

The frequency range of the STAFF experiment is a priori more suitable for studying the proton foreshock than the electron foreshock. However, waves at  $\sim 1$  Hz called 'upstream propagating whistlers' have been detected in front of the ion foreshock, in the electron foreshock (Russell et al., 1971). The origin of these waves is still controversial: they could be anisotropy-driven instabilities amplified locally by electrons (Sentman et al., 1983) or they could be generated at the shock itself by the ions and then propagate upstream (Krauss-Varban et al., 1995). Data from the four STAFF experiments will allow the source to be localised and, together with four point measurements of the particle distribution function, should allow this question to be answered. Also in the electron foreshock, possible non linear mode coupling between Langmuir waves and whistler mode waves can be investigated by combining Whisper and STAFF spectrum analyser measurements.

Entry into the ion foreshock is accompanied by the onset of strong electrostatic noise in the frequency range from about 100 Hz to 10 kHz, often called 'ionacoustic' noise. This noise is associated with 1-40 keV ions streaming into the solar wind (Gurnett, 1985). The identification of the mode of propagation of this noise requires a better description of the surrounding plasma. Deep inside the ion foreshock, the bulk flow velocity of the solar wind is found to be reduced by 5 to 10% (Zhang et al., 1995); in a collisionless medium, this can only be a consequence of wave-particle interactions. The electric field spectrum from the STAFF spectrum analyser will allow the complete spectrum, from the EFW to Whisper frequencies, to be measured, thus fully describing this noise. It is well known that different kinds of waves (Greenstadt et al., 1995) are related to the shape of the different kinds of upstream ion distribution functions observed in the ion foreshock (Fuselier, 1995). Using the four point measurements, waves can be used to probe the ambient plasma and help localise the sources of reflected and diffuse upstream ions. Numerical simulations demonstrate the close connection between diffuse ions and, upstream waves, and their effect on the solar wind (Scholer, 1995).

A new class of ULF waves (with frequency  $\sim 0.3$  Hz) upstream of the bowshock has been discovered by Le *et al.* (1992) when the solar wind plasma  $\beta$  is high. Neither the intrinsic wave mode nor the free energy source have yet been determined unambiguously. In regions where  $\beta$  is particularly large these waves appear to be ion cyclotron waves (Le *et al.*, 1992). A careful analysis of waves in the same frequency range, but when the solar wind plasma  $\beta$  is low (<1), has led Blanco-Cano and Schwartz (1996) to conclude that these waves are extended whistler mode trains. The mode of these waves can be unambiguously determined by the use of the waveform data from four spacecraft. Comparison with particle data obtained simultaneously should indicate the source of the free energy responsible for their amplification.

## 2.2. The Earth's bow shock

Upstream of the quasi-parallel bow shock, ULF waves steepen to form shocklets and Short Large Amplitude Magnetic Structures (SLAMS); and high-frequency whistler wave packets are amplified. Because their phase velocity is less than the solar wind flow speed, the majority of the waves in the foreshock must eventually be convected back into and through the shock itself. This implies that the foreshock and the shock cannot be treated separately (Burgess, 1995). The dominant instabilities and the two-dimensional scales found in numerical simulations (Dubouloz and Scholer, 1995) must be compared with the four-point observations of STAFF. The notion of cyclical shock reformation has been investigated by simulations of high Mach number quasi-parallel shocks (Winske *et al.*, 1990). This work prompts the following questions which should be answered using Cluster wave measurements: What is the role of high-frequency waves in the cyclical reformation? Which kind of turbulence is associated with non-gyrotropic ion distributions observed in space and simulations at shocks?

Similarly, recent simulations of supercritical quasi-perpendicular shocks have shown that shock-reflected ions generate upstream propagating whistler waves at frequencies of the order of a few tens of Hz in the plasma rest frame (Hellinger et al., 1995; Krauss-Varban et al., 1995). These waves propagate obliquely with respect to both the shock normal and the local magnetic field and are most intense in the shock ramp. This suggests that quasi-perpendicular shocks are intrinsically three-dimensional, a conjecture which should be tested byusing four-point STAFF measurements, especially when operating in burst mode which yields the waveform up to 180 Hz. Simulations also suggest that electron heating through quasi-perpendicular shocks is essentially adiabatic except for some slight heating by the upstream whistlers, and eventually by lower hybrid waves located within the main shock transition (Krauss-Varban, 1994; Savoini and Lembège, 1995). While whistler waves have been extensively observed, the identification of waves near the lower hybrid resonance frequency (typically in the range from about 3 to 15 Hz) is almost non-existent, due to the inappropriate frequency ranges of electric and magnetic sensors on previous missions (Scudder et al., 1986). A detailed analysis of the waves detected with Cluster instruments in the shock may give evidence of lower hybrid waves and their relationship to the whistler mode turbulence, and even to the low-frequency electromagnetic noise. In the downstream region, characteristic electron distributions have been observed; they require a more efficient non-adiabatic heating process (Veltri et al., 1990; Savoini and Lembège, 1995). Savoini and Lembège (1994) have reported magnetised simulations that reproduce simultaneously both the observed flat-topped electron distribution functions and the electromagnetic shock structure. Nevertheless, the origin of the non-adiabatic heating is not completely elucidated; it is probably intimately related to the frequently observed shock-associated higher frequency waves. These waves lie in the kHz frequency domain and will be detected easily by STAFF. Multi-spacecraft

observations will provide useful information on the relation between local shock structure and wave intensity and, in particular, the possible relationship between the intensity of the high-frequency waves and the thickness of the bow shock.

Finally, one of the main objectives of Cluster is to determine unambiguously the frame-dependent wave properties such as frequency, phase and group velocities in the strongly Doppler-shifted environment of the solar wind. Four satellites will help identify the different kinds of waves which are being amplified or which can propagate to a given measurement point. So far very few determinations of the coherence length of the turbulence have been published (Le *et al.*, 1993); filling this gap in our knowledge is certainly one of the main tasks of Cluster. The variation of the Cluster inter-spacecraft separation during the course of the mission, and the changing geometrical configuration, will enable different wavelength ranges to be studied.

## 2.3. The magnetosheath

The full importance of the role played by the magnetosheath in the interface between the free solar wind and the magnetosphere is gradually being recognised. The magnetosheath is a magnetofluid in which the flow and magnetic field patterns change from the bow shock to the magnetopause; a slow mode transition region has been identified and plays a crucial role in these changes (Song, 1994). The properties of the plasma in the outer magnetosheath depend on the bow shock properties, while the properties of the plasma of the inner sheath depend on the shear angle between the magnetosheath magnetic field and the geomagnetic field (Phan *et al.*, 1994).

The dissipation processes are not the same in different regions of the magnetosheath. Using one or two spacecraft, several wave modes have been identified, at scales larger than or equal to the ion Larmor radius (Hubert, 1994; Lacombe and Belmont, 1995). Anticorrelation is observed between the proton temperature anisotropy and the proton  $\beta$  in the sheath depletion layer (close to the magnetopause) when the magnetosheath is strongly compressed; this probably indicates a quasi-linear equilibrium reached through unstable mirror and Alfvén ion cyclotron waves (Anderson *et al.*, 1994). The bow shock, the inner sheath, and the magnetopause can all affect the waves convected from the solar wind to the magnetosphere, through mode coupling, damping, mode conversion and reflection (Hubert, 1994; Krauss-Varban, 1994). For deterministic reasons, information must also propagate from the inner to the outer magnetosheath, but the nature of its transmission is still an open question.

Microscale plasma phenomena are critical in this high- $\beta$  plasma. In particular, whistler-mode noise is known to play an important part in controlling electron thermal anisotropy.

## 2.4. The magnetopause and the low-latitude boundary layer

There is ample indirect (and some direct) evidence that the magnetopause is a permeable boundary. The investigation of the physical processes by which mass and momentum are transferred through the magnetopause, from the solar wind to the magnetosphere, is one of the prime goals of the mission. Our objective is to assess the role that plasma waves play in affecting and controlling these transfers.

Different models have been proposed, such as the reconnection model or the Kelvin-Helmholtz instability. Also, there is evidence for localised flux tubes, known as Flux Transfer Events (FTEs), connecting the magnetosheath to the magnetosphere, but whether FTEs are the remnants of reconnection events or the nonlinear consequence of tearing or Kelvin-Helmholtz instability is still an opened question. Hence, for all models, the key issue is the identification of the plasma waves that permit the anomalous cross-field diffusion and/or resistivity at a global/local scale. Many experiments aboard single spacecraft have shown that a very high level of fluctuations is observed in all frequency ranges during magnetopause crossings (Labelle and Treumann, 1988; Anderson et al., 1991; Cattell et al., 1995). The estimation of diffusion coefficients indicate that the ULF fluctuations are the more likely to provide the anomalous diffusion (Gendrin, 1983). Nevertheless the question of the origin of these fluctuations has seldom been addressed in the literature. Two different hypotheses can be considered: either they are due to local instabilities of the boundary, or they are generated in the magnetosheath and are amplified at the magnetopause. The second hypothesis has been tested on a simple model by Belmont et al. (1995). This study has shown that most of the experimental characteristics of the fluctuations observed in this region (Rezeau et al., 1989) can be explained by the resonant amplification of magnetosheath fluctuations at the magnetopause. These results are encouraging but they should be confirmed by including more realistic characteristics of the magnetopause in the model. The STAFF experiment will permit a detailed comparison of the magnetosheath and magnetopause fluctuations with very high resolution four-point measurements. It will be possible to compare data recorded at the same time in the magnetosheath, the magnetopause and the magnetosphere, and thus hopefully confirm this theoretical interpretation. Moreover, when observing the same wave event aboard the four spacecraft, the mode identification can be done unambiguously, without any a priori hypothesis.

#### 2.5. The cusp

Because of its singular magnetic field configuration, the cusp is thought to be one of the regions where magnetosheath plasma entry occurs. In spite of the key role it may play, the exterior cusp is one of the less explored regions of space that Cluster will visit. From a few crossings by the HEOS spacecraft (Haerendel et al., 1978), it has been inferred that the flow in the cusp region shows very

turbulent behaviour. At lower altitudes, but still R > 2  $R_E$ , strong field-aligned currents were observed by the OGO-5 spacecraft. These current sheets or filaments were found to be accompanied by Ion Cyclotron Waves (ICWs) and by higher frequency waves, which are presumably electrostatic (Fredericks *et al.*, 1973). The wave characteristics of the cusp region are relatively unexplored, and the complete frequency coverage of the Wave Experiment Consortium is particularly desirable. Furthermore, the STAFF experiment ability to perform spatial correlation of waveforms at lower frequencies, and comparison of spectra at higher frequencies, will help characterise the plasma waves or turbulence, and hence allow the study of their role in accelerating particles along the magnetic field lines.

#### 2.6. The plasmasheet

The central part of the magnetotail, the plasmasheet, is a very complex region where the plasma is accelerated up to tens of keV; this acceleration is particularly efficient during substorms. We are still far from a full understanding of the processes that lead to the reconfiguration of the tail magnetic field and to the acceleration and Earthward injection of plasma during substorms. At least, there is as yet no consensus on a scenario explaining this chain of processes. One of the key questions is the relation between dipolarisation/injection occurring in the inner plasmasheet, and the signatures observed further out in the tail-like flux ropes and/or plasmoids. In a plasma where binary collisions are essentially absent, the dramatic topology changes mentioned above are controlled by collisionless processes. There are two types of collisionless processes involving breakdown of adiabatic invariants: (1) waves and turbulence at frequencies of the order of the gyrofrequency or of the order of the bounce frequency, and (2) non-adiabaticity associated with curvature effects within thin current sheets. In fact, these two types of processes are related, as will be seen below. The coordinated measurements to be carried out aboard the four Cluster spacecraft will provide a powerful new tool to study the role played by these two kinds of processes.

It is well known that the first adiabatic invariant may not be conserved in the tail, at least for ions, and possibly for electrons. This loss of adiabaticity makes it more difficult to describe transport in the tail. Büchner and Zelenyi (1988) have proposed to use the parameter  $\kappa$  to classify the various types of orbits;  $\kappa$  is the square root of the ratio between the curvature radius and the ion Larmor radius, and the usual adiabatic invariants are conserved in regions where  $\kappa \gg 1$ . The transition to a chaotic regime can have important macroscopic consequences; for instance, it has been suggested that it could play a key role as a substorm trigger. Delcourt *et al.* (1995) have investigated the transition from the adiabatic to the chaotic regime. Using a simple analytical model of short-lived centrifugal impulses and simulation of particle motion, they also showed that the  $\kappa=1$  regime is characterised by prominent bunching effects in gyration phase, which can lead to the formation of non gyrotropic distributions. In turn, these distributions

can be strongly unstable, thereby leading to the generation of intense plasma waves around the proton gyrofrequency: this hypothesis should be tested with simultaneous Cluster measurements of waves and particles.

Thin Current Sheets (TCS) have been observed in the central part of the plasma sheet (see for instance Mitchell et al., 1990). A direct relation between the thinning of TCS and substorm break up has been evidenced in a number of cases (see, e.g., Lui et al., 1992; Perraut et al., 1995). Other triggers can be involved, however. Lui et al. (1992) and Perraut et al. (1993) have shown that intense waves are observed just prior to break up or at break up. These waves have frequencies typically in the proton gyrofrequency range. These measurements were carried out relatively close to the Earth. Nevertheless there are observations made at larger distances by Galileo and Geotail: Galileo measurements (Khurana et al., 1995) confirm that flux ropes and thin current sheets also develop in the far plasma sheet; small scale structures are regularly observed inside the plasmasheet with Geotail (Matsumoto et al., 1994), associated with broad band electrostatic noise (BEN). Therefore turbulence can play a role in triggering substorms. The assessment of this role requires the spatial coverage that will become available with Cluster.

At lower frequencies or larger scales, the existence of small-scale Field-Aligned Current (FAC) structures has been inferred from GEOS measurements (Robert et al., 1984). While interesting, these observations carried out aboard a single spacecraft remain inconclusive because spatial and temporal variations cannot be separated. The electric and magnetic measurements on-board the four Cluster spacecraft will allow the removal of this ambiguity for the first time, and hopefully this will clarify the link between these FACs and nonlinear Kinetic Alfvénic Structures (KAS). During the preparation of the mission, techniques have been developed to fully characterise the small-scale FAC/KAS, based on the measurements that will be carried out by WEC and by other experiments aboard the four satellites. These techniques involve: (1) inter-spacecraft correlations, (2) wavelet analysis, adapted to varying distances between the spacecraft, and/or to spatial scales determined from data obtained from other experiments, both within and outside WEC, (3) singular spectrum analysis (Vautard et al., 1992) to help characterise localised structures, and (4) sophisticated methods to determine the 'k' spectrum from four points. These methods have been developed in close collaboration with (and tested by) the European Network on Numerical Simulation.

## 2.7. The auroral region

The present plan for Cluster data acquisition makes it possible to investigate the auroral zones, with the four satellites crossing this region close to perigee. Cluster will be at a rather high altitude (above  $4 R_E$ ) and thus will not cross the most 'active' auroral region, i.e., the region where data from Viking suggest that most of the parallel acceleration and non thermal radiation take place (Louarn *et al.*, 1990). Nevertheless the physical conditions that prevail above, and below, the

'main' acceleration region are very important; they fix the boundary conditions, and therefore control the parallel acceleration. Studies of the region below the main acceleration region, using Freja data (Wahlund et al., 1994) have produced evidence for small-scale field-aligned current structures, identified as Solitary Kinetic Alfvén Waves (SKAWs), by Louarn et al. (1994). Preliminary results show that the parallel electric fields of the SKAWs are quite large, thus suggesting that they might play a role in the acceleration process. It is interesting to study the field aligned currents and the SKAWs at higher altitudes, to determine their possible role in the direct acceleration of particles, and the determination of boundary conditions. Given the small transverse scale of the SKAWs, and the large Doppler shift associated with the spacecraft motion, this study is quite difficult. More generally small scale field aligned currents, be they stationary or unsteady (Alfvén waves) are important at these altitudes ( $\sim 4~R_E$ ). Waveform measurements to be carried out aboard the four spacecraft as they pass by, one after the other, will allow an appropriate characterisation of these structures. It is important that the magnetic field, during these periods, will be approximately in the spin plane, which helps the determination of the parallel electric field of the SKAWs. At higher frequencies large amplitude electrostatic waves, presumably ion acoustic waves, should be observed, in close association with the SKAWs. The STAFF Spectrum Analyser is well suited to investigate these waves, which should have frequencies below the ion plasma frequency. Correlations between STAFF and the particle experiments will help in assessing the role of these waves in accelerating particles. In the acceleration region, electromagnetic ion cyclotron waves in the ELF frequency range (some 100 Hz) have been observed (Temerin and Lysak, 1984); they are presumably generated by accelerated electrons beams. Will they be observed at higher altitude? More generally very few, or even no measurement of electromagnetic waves has been performed yet in the high latitude auroral zone, and STAFF measurements will be somewhat exploratory here.

## 3. Scientific Wave Data Analysis

The innovation of the Cluster project is that, for the first time, a set of four identical spacecraft will produce a powerful tool for disentangling spatial and temporal variations. This has led the STAFF team to prepare specific tools to analyse the wave data. Some are discussed below, together with the method applied to validate the on-board analysis performed by the STAFF spectrum analyser.

The current structures which Cluster will encounter will normally be characterised by the Fluxgate Magnetometer (FGM). Nevertheless, some of these structures are of very small scale, corresponding to temporal signatures of the order of 1 s or less (Rezeau *et al.*, 1993). In such cases, the search coil data are complementary to FGM ones, STAFF being more sensitive for frequencies greater than about 1 Hz. When a small-scale structure, such as a small-scale current tube or a solitary

wave, is observed by one spacecraft, the immediate question is whether the other spacecraft observed the same structure? To answer this question we must be able to identify that the different signatures possibly observed aboard two, three or four spacecraft do correspond to the same structure. A two-spacecraft study of magnetic fluctuations at the magnetopause has been performed with ISEE data. It has shown that in some cases the same structure can be identified on ISEE-1 and -2 (Rezeau et al., 1993). Nevertheless, the most simple method of identification, the computation of the correlation function of the two signals, proved to be difficult to use for turbulent signals as observed at the magnetopause. The reason is that the correlation is efficient for identifying the same frequency in the two signals. This has two major consequences: (i) as the spectrum of the fluctuations is a continuous spectrum, a given frequency is always present in the data and the correlation coefficient is never very small, (ii) there is a perspective effect: a given structure will have a typical frequency which is different on two spacecraft, if the distance of closest approach is different (Rezeau et al., 1990, 1993) and thus the two signatures will appear weakly correlated. In conclusion, the correlation will be efficient only in the cases when the inter-spacecraft distance is small and the conditions of observation of a given structure are similar on both spacecraft. But, as in a more general context it does not work, we are now developing a new tool for inter-spacecraft correlation.

Plasma waves will be characterised by complementary means involving ground-based and on-board calculations of the auto- and cross-correlation functions, as well as inter-correlation between waveforms measured at the various spacecraft locations.

From auto-correlations the energy density of electric and magnetic components will be inferred, together with the electrostatic/electromagnetic nature of the observed waves. The full knowledge of the polarisation characteristics of an electromagnetic wave field requires the computation of the cross-power spectra. Assuming knowledge of the dispersion relation, the Wave Distribution Function (WDF) is determined from the auto- and cross-power spectra at a given spacecraft location (Lefeuvre et al., 1981). The WDF approach allows to remove the sign ambiguity in the wave normal direction (parallel or anti-parallel to the Earth magnetic field) when the measurement of at least one electric component is added to the measurements of the three magnetic components of the wave field. Depending on the frequency range of the waves studied, the spectral matrix will be calculated either on the ground from the waveform data, or on-board each spacecraft by the STAFF spectrum analyser (see next section). Using the waveform measurements from the four spacecraft a generalised spectral matrix containing all the available auto-, cross- and inter-spacecraft power spectra can be computed. From it, the Field Energy Distribution (FED) function will be determined which specifies how the field energy is distributed in a four dimensional space, i.e., as a function of the frequency and the three components of the wave vector, without assuming any dispersion relation (Pinçon and Lefeuvre, 1991). This kind of measurement will be achieved for the first time, thanks to the simultaneous measurements at four

locations. To compute on the ground the general spectral matrix, we will need both the STAFF search coil data and the electric field waveform from the EFW experiment (Gustafsson *et al.*, this issue). This will yield five components of the electromagnetic waves on each spacecraft. STAFF and EFW hardware have been designed to simplify this correlation: the low pass filters are identical, the sampling frequency is the same, and a synchronisation signal for simultaneous sampling is sent to both experiments by the DWP experiment (Woolliscroft *et al.*, this issue). In addition, it is possible to use electric field measurements from the Electron Drift Instrument (EDI) (Paschmann *et al.*, this issue). The combination of data from the EFW, EDI and the search coil will allow the determination of the six components of the electromagnetic field. The inter-experiment link between STAFF and EDI will allow to synchronise EDI and WEC data.

The WDF strongly depends upon the geometry of the ray from the source to the point of observation. Simultaneous measurements at the various spacecraft locations will allow triangulation via multiple ray-tracing calculations, thus permitting the study of source location. An application of this method has been performed in order to validate the STAFF spectrum analyser calculations (Santolik, 1993; Belkacemi, 1993, 1994). An example, using a known simulated input signal and data output from one satellite, is shown in Figure 1, where the error in the determination of the wave normal direction is studied as a function of the signal-to-noise ratio. The WDF method applied here to recover the input direction of the injected signal has been compared with two other methods (Means, 1972; McPherron *et al.*, 1972) which can be used when the wave is assumed to be planar. Several independent realisations of noisy samples have been used to calculate the spectral matrices. Except at high signal to noise ratios, it is observed that the wave normal direction  $(\theta \text{ and } \phi)$  is well recovered with the three methods.

The FED function calculation method has been applied to simulated data, under different conditions: number of wave components, respective spacecraft location, frequency and signal to noise dependence (Pinçon and Lefeuvre, 1992). This has allowed the determination of the experimental constraints under which the FED function can be determined. In particular, a study by Pinçon *et al.* (1990) has shown the influence of the inter-spacecraft distance on the results (see Figure 2); valid results will be obtained whenever one of the maximum inter-spacecraft distances is less than five times the minimum one.

An extensive characterisation of waves by Cluster needs, as seen above, correlative studies with data from different experiments. It is planned that all WEC Co-Investigators will have access to all WEC high-resolution data, through a common data analysis system, ISDAT (Pedersen *et al.*, this issue). Correlative studies with non-WEC experiment are foreseen, first through the Cluster Science Data System (CSDS) in which STAFF and all the other Cluster teams participate (Schmidt and Escoubet, this issue), second using case-by-case high-resolution data.

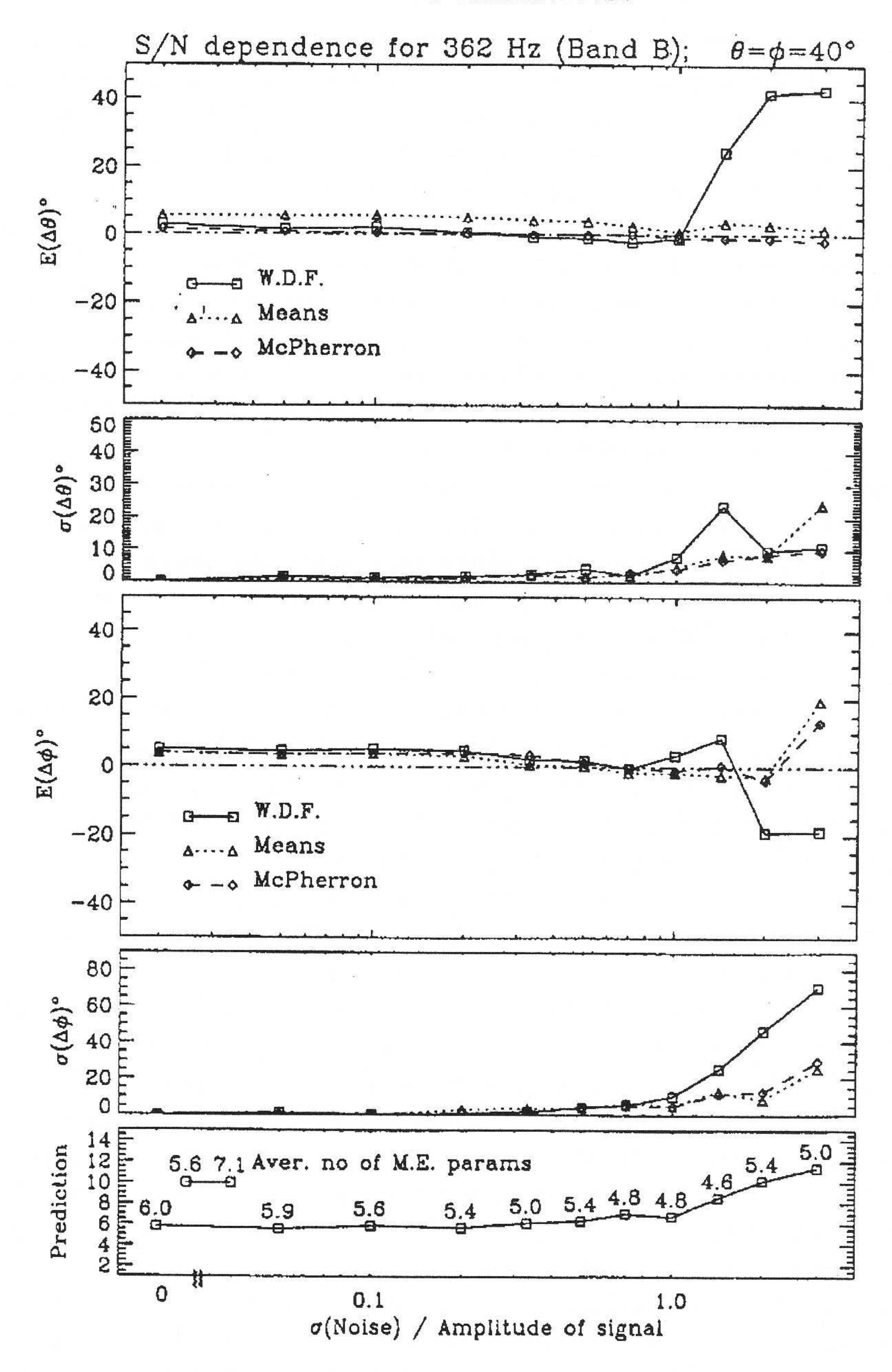


Figure 1. Electromagnetic plasma waves are simulated, using Maxwell equations. For a given plasma (here  $f_p=100~{\rm kHz}$  and  $f_{ce}=6~{\rm kHz}$ ), the ratio between the variance of the random noise added to the electromagnetic field waveform and the signal is varied. The wave normal direction is fixed and known ( $\theta=40^\circ$ ,  $\phi=40^\circ$ ). These two angles are estimated by the spectral matrix calculated with a simulation of the STAFF spectrum analyser. From the top to the bottom, the panels of the figure give the average value of the angle error  $E(\Delta\theta)$ , the corresponding standard deviation  $\sigma(\Delta\theta)$ , the average value of the angle error  $E(\Delta\phi)$ , the corresponding standard deviation  $\sigma(\Delta\phi)$ , and a prediction parameter used to qualify the WDF solutions (see Lefeuvre et al., 1981), as function of the signal to noise ratio. The squares refer to the WDF method, the triangles to the Means' method, and the diamonds to the McPherron's method. The figure gives the angle errors  $\Delta\theta$  and  $\Delta\phi$ , that is always less than  $10^\circ$ .

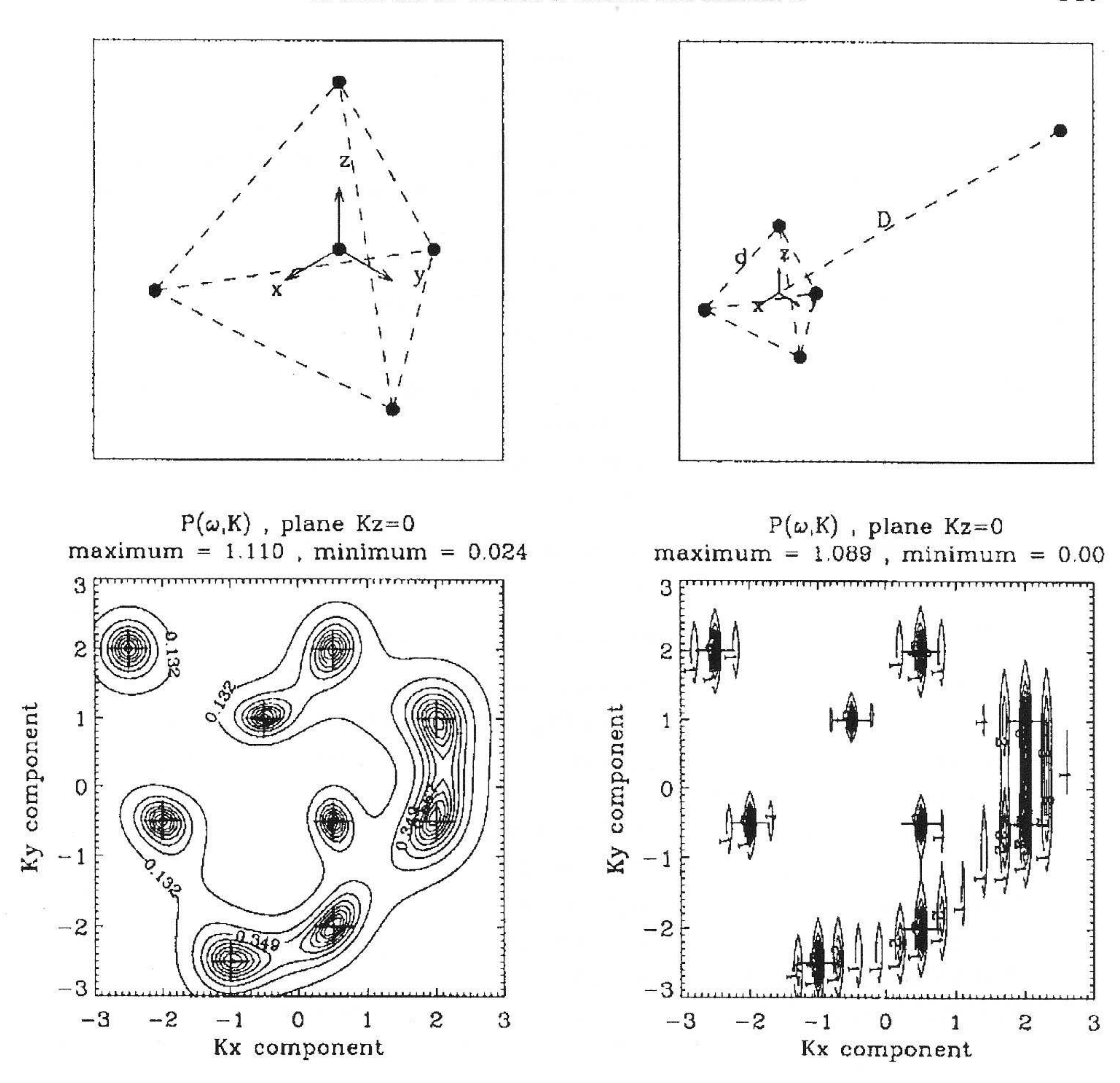


Figure 2. Example of the Field Energy Distribution (from Pinçon et al., 1990). For a given distribution, here nine plane waves, the calculation of the FED is performed for different spacecraft respective position (top panels). Four satellites are located at top of a tetrahedron. On the left, the fifth satellite is added at the centre of the tetrahedron, whereas on the right the fifth satellite is placed at a large distance from the centre of the tetrahedron. The results derived from the 5 satellites are respectively given in the bottom panels as energy contours in the kx, ky plane for kz = 0. The initial FED is represented by crosses. The results are good when the fifth satellite is inside the tetrahedron (left case) or at distances D of the same order of magnitude as d. Differences arise when D is large relatively to d (right case, the ratio of distances is 20) (after Pinçon et al., 1990). The results are similar with four spacecraft.

# 4. Experiment Technical Description

The STAFF experiment comprises a boom-mounted three-axis search coil magneto-meter and two complementary data-analysis packages: a digital spectrum analyser, and an on-board signal-processing unit. The latter permits the observation of the three magnetic waveforms up to either 10 Hz or 180 Hz, depending upon mode. The spectrum analyser also receives the signals from the four electric field probes

## Table I Group tasks

CETP	STAFF co-ordination (PI + technical manager) manufacturing and testing of: search coil, magnetic waveform unit, calibration check-out software support to integration and testing data analysis		
DESPA- Meudon	manufacturing and testing of the spectrum analyser check-out software support to integration and testing data analysis		
LPCE-Orléans	design, calibration and tests of the filters data analysis		
SSD-ESTEC	manufacturing of the filters		
CEPHAG Co-Is from	theoretical support for data analysis relationship with ground-based measurements link between STAFF and the other WEC experiments		
other institutes:			
LPCE, Orléans, France	P. M. E. Décréau		
Sussex University, U.K.	M. P. Gough		
University of Iowa, U.S.A.	D. A. Gurnett		
SISP, Uppsala, Sweden	G. Gustafsson		
SSD-ESTEC, The Netherlands	A. Pedersen		
Sheffield University, U.K.	H. St. C. Alleyne, L. J. C. Woolliscroft		

of the EFW experiment, which are used to form a pair of orthogonal electric field dipole sensors. All five inputs  $(2E + 3 \times \mathbf{B})$  are used to compute in real time the  $5 \times 5$  Hermitian cross-spectral matrix at 27 frequencies distributed logarithmically in the frequency range 8 Hz to 4 kHz.

STAFF is one of the five experiments of the Wave Experiment Consortium (WEC) (see Pedersen *et al.*, this issue). The STAFF team includes scientific and hardware contributions from a number of institutes, as shown in Table I. To optimise coordination within WEC, the STAFF investigator team includes all the WEC Principal Investigators.

## 4.1. The search coil sensors and the pre-amplifier

Three mutually orthogonal sensors are mounted on a rigid boom away from the spacecraft body (see Figure 3). Two sensors,  $B_y$  and  $B_z$ , lie in the spin plane and are aligned mechanically with the long wire dipole antennas of the EFW experiment; the third is parallel to the spacecraft spin axis. Each sensor consists of a high

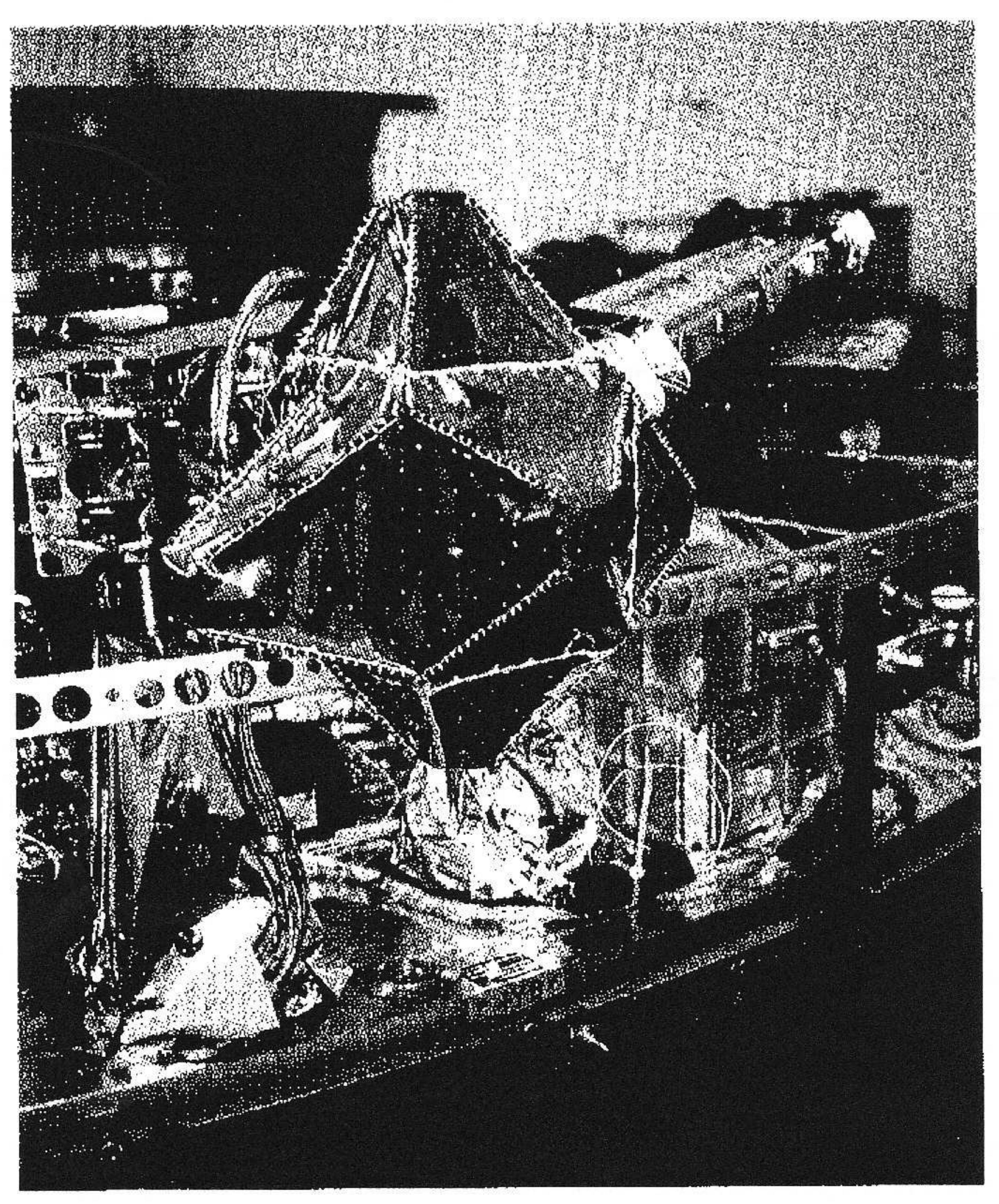


Figure 3. One set of the 3 STAFF search coil antennas under their thermal blanket, on the FM1 spacecraft.

permeability core embedded inside two solenoids. The main winding has a very large number of turns mounted in separate sections. The frequency response of the sensor is flattened in the frequency range 40–4000 Hz by a secondary winding used to introduce flux feedback. The secondary winding is also used as a calibration loop on which an external AC signal is applied through a calibration network included in the pre-amplifiers. The search coils are designed so as to minimise their sensitivity to electric fields. The transfer function and the experiment sensitivity are given in Figure 4. The measured sensitivity is  $3 \times 10^{-3}$  nT Hz  $^{-1/2}$  at 1 Hz and  $3 \times 10^{-5}$  nT Hz  $^{-1/2}$  at 100 Hz. The similarity of the search coils mounted on the four spacecraft is good, as can be seen on lowest panel of Figure 4 which gives the difference between two models of the uncalibrated amplitude and phase responses of one component  $(B_x)$ : the phase is reproductible within  $\pm 1^{\circ}$ , and the amplitude within 0.2 dB above 1 Hz, at the exception of the vicinity of 50 Hz. Much the same result is obtained for any combination of sensors.

In order to compare accurately data from the four satellites, a careful measurement of the angle between each magnetic axis and its corresponding mechanical

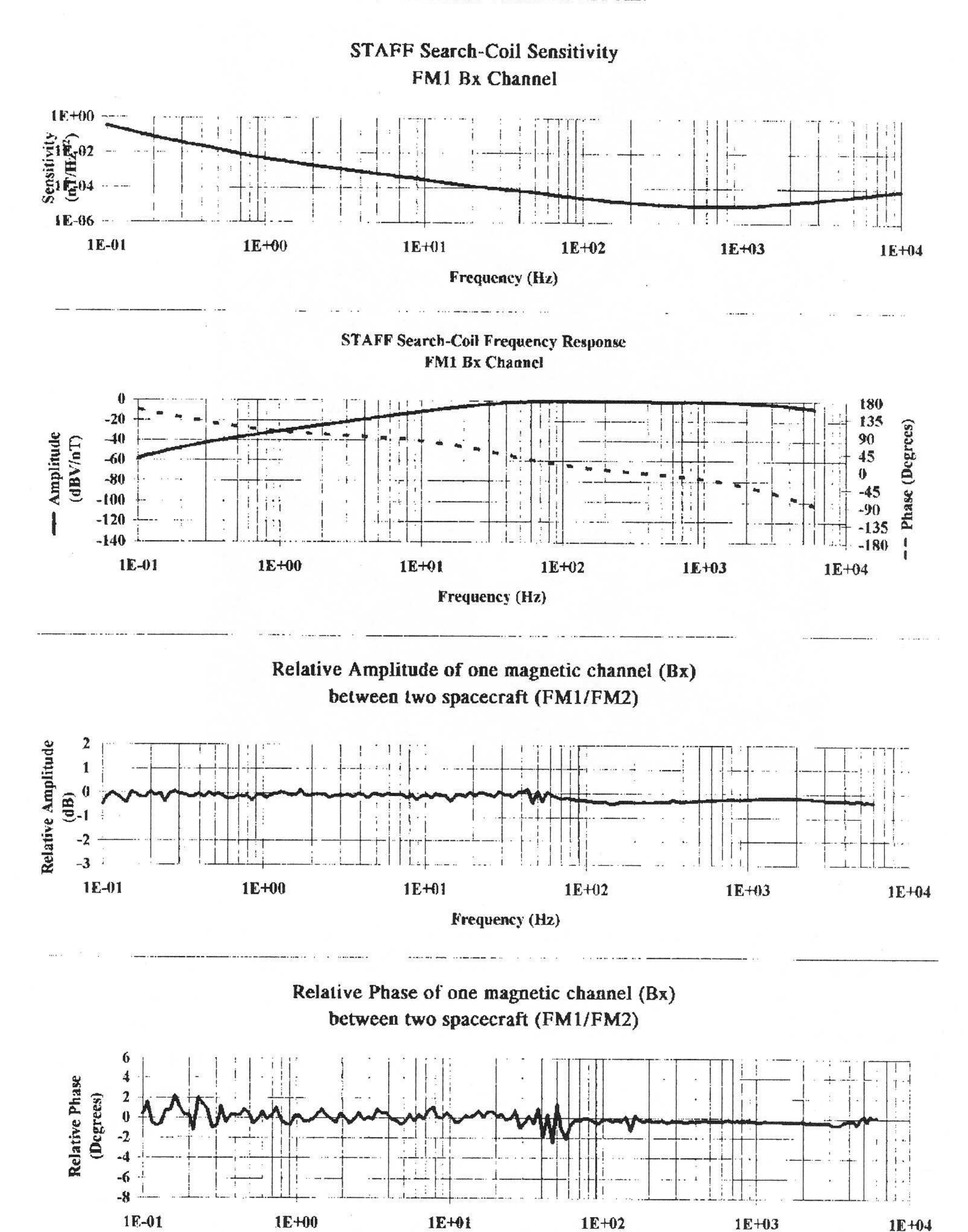


Figure 4. STAFF search coil and pre-amplifier transfer function and sensitivity measured in calibration facility at Chambon la Forêt, France. Upper panel: Flight Model 1 sensitivity for the  $B_x$  channel. second panel: transfer function for the same antenna in amplitude and phase. Bottom panels: example of the similarity of the search coil on-board the four spacecraft, the relative amplitude and phase responses of channel  $B_x$  on-board spacecraft 1 and 2.

Frequency (Hz)

1E+04

axis has been made. These angles may be a few degrees, but they are known with a precision of 0.1°. Thus the magnetic field may be accurately transformed into any required reference frame.

Three pre-amplifiers are mounted in an electrical unit, located on the spacecraft deck. The low-power-consumption pre-amplifiers have a low-noise input stage and high-input impedance since they are connected to the magnetic sensors which are characterised by a low DC resistance and a very high impedance in the vicinity of the resonant frequency. The dynamic range of the pre-amplifiers is about 100 dB, which allows weak signals to be measured in the presence of the large voltage signals induced by the rotation of the spacecraft in the DC magnetic field. A new pre-amplifier using hybrid technology has been developed (Youssef *et al.*, 1991) and will be flown for the first time on Cluster. This technique has the advantages of including protection against radiation, the possibility of thermal control of the pre-amplifier, while being lighter than more traditional technology.

The output signals of the magnetic pre-amplifiers are conditioned for use at frequencies below 180 Hz by (i) the magnetic waveform unit, and for use up to 4 kHz by (ii) the spectrum analyser, (iii) the Wide-Band Data unit, (iv) the EFW experiment for the fast event detector, and (v) the EDI experiment.

#### 4.2. The magnetic waveform unit

The magnetic waveform unit (see Figure 5) consists of three sections which assure respectively: waveform digitalisation, data output interface, and on-board calibration. The latter is discussed in Section 4.4.

The three magnetic components  $B_x$ ,  $B_y$ ,  $B_z$ , at the output of the search coil pre-amplifier are passed through low-pass anti-aliasing filters with -3 dB cut-off at either 10 Hz or 180 Hz. These filters are of seventh order, i.e., they have an attenuation of 42 dB per octave. They are stable to better than 1% in amplitude and 1° in absolute phase; comparison between the different spacecraft show that they maintain this accuracy. The sampling frequency is 2.5 times the filter frequency, 25 or 450 Hz. Thus, the rejection of aliased components is at least 40 dB. Identical filters are used in the EFW experiment so as to optimise the correlation of electric and magnetic waveforms.

The filtered signals are applied to three sample and hold devices synchronised by the DWP experiment, then digitised, and sent to the DWP experiment. The same synchronisation signal is sent to both the STAFF and the EFW experiments. The bandwidth for the waveform measurements is selected by telecommand. The filtered signals are simultaneously sampled in a large dynamic range within a very short sampling time of about 10  $\mu$ s in order to guarantee a relative error of less than one degree at 180 Hz between the three components. The sampling signal, provided by DWP, is common between the STAFF and EFW experiments in order to ensure the best simultaneous analysis of the five available components of the electromagnetic waves.

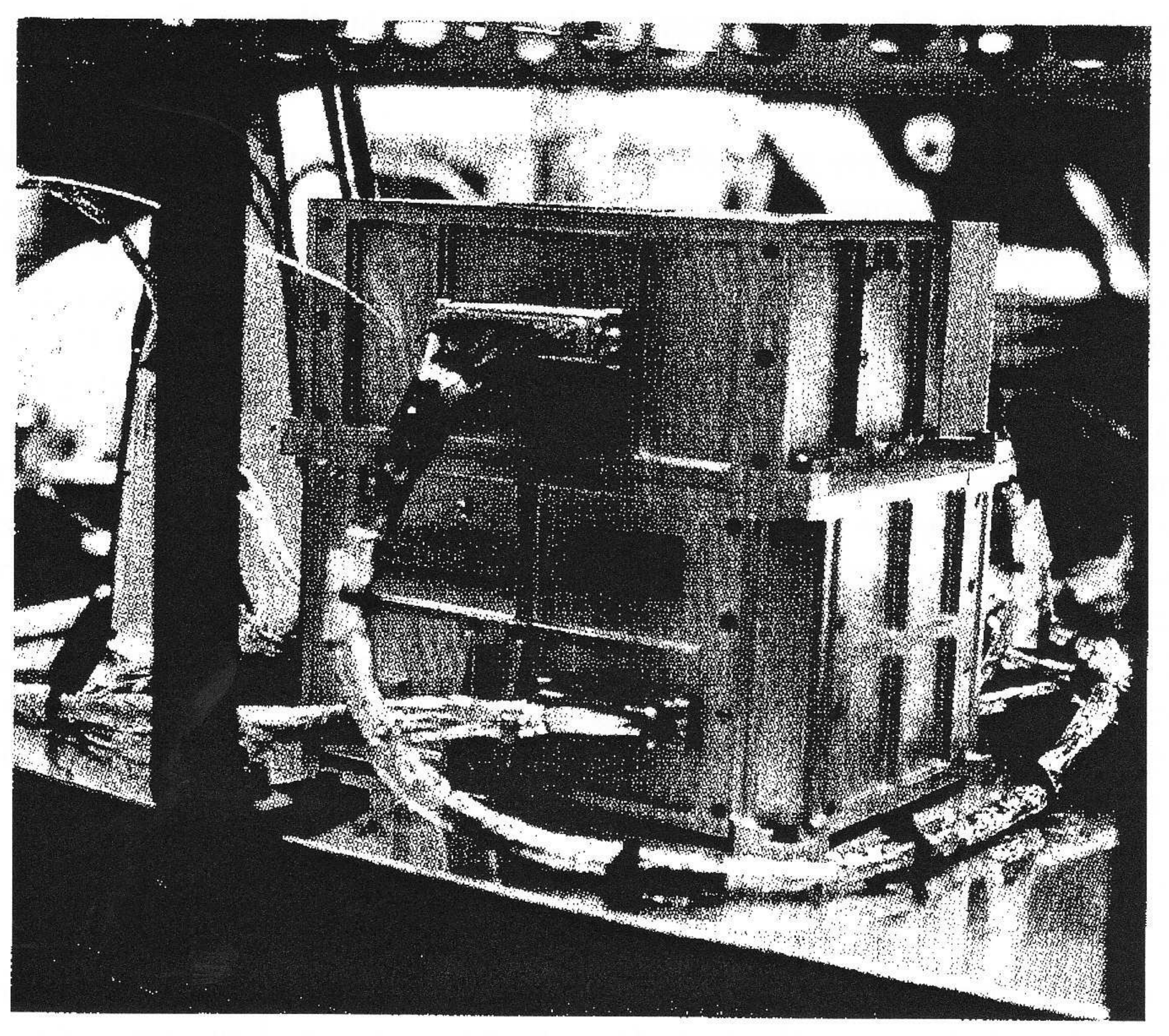


Figure 5. The STAFF electronic box on the Cluster platform at Dornier (WEC 8/1, the waveform unit is on top of WEC 8/2, the spectrum analyser) for the flight model number 4.

The samples are digitised in a real 16-bit analogue-to-digital converter and transmitted to the DWP experiment through one parallel interface. The 16-bit digitalisation allows to analyse simultaneously natural waves of a few  $10^{-5}$  nT Hz<sup>-1/2</sup> and the large signal induced by the rotation of the spacecraft in the environmental DC field, up to some 100 nT at 0.25 Hz. With such a dynamic we expect to have accurate measurements, even at the inversion of the DC magnetic field at the magnetopause.

Owing to telemetry limitations, a reduction of the dynamic data range from 16 to 12 bits is performed inside DWP (Woolliscroft *et al.*, this issue). The principle is to transmit the full 16-bit word at the beginning of each telemetry packet, and later the difference between the successive samples, coded on 12 bits in such a way that the dynamics of the experiment should be preserved even at boundary crossings. Conservative back-up solutions can be selected by telecommand, being either a more crude compression, or no compression at all. The back-up compression will be used for instance at perigee where the spin signal is expected to be above some 200 nT.

## 4.3. THE SPECTRUM ANALYSER

The spectrum analyser calculates the complete auto- and cross-spectra of three components of the magnetic and two of the electric field, over a frequency range of nine octaves, with commendable time resolution. More precisely, the spectrum analyser determines the complete  $5 \times 5$  Hermitian cross-spectral matrix of the signals from five input channels, over the frequency range of 8 Hz to 4 kHz, as follows (Figure 6).

The five auto-spectral power estimates are obtained with:

- a dynamic range of approximately 100 dB,
- an average amplitude resolution of 0.38 dB,
- a sensitivity as shown in Figure 4 for the magnetic components and in Gustafsson *et al.* (this issue) for the electric components.

The 10 cross-spectral power estimates are normalised to give the coherence, which is obtained with the following precision:

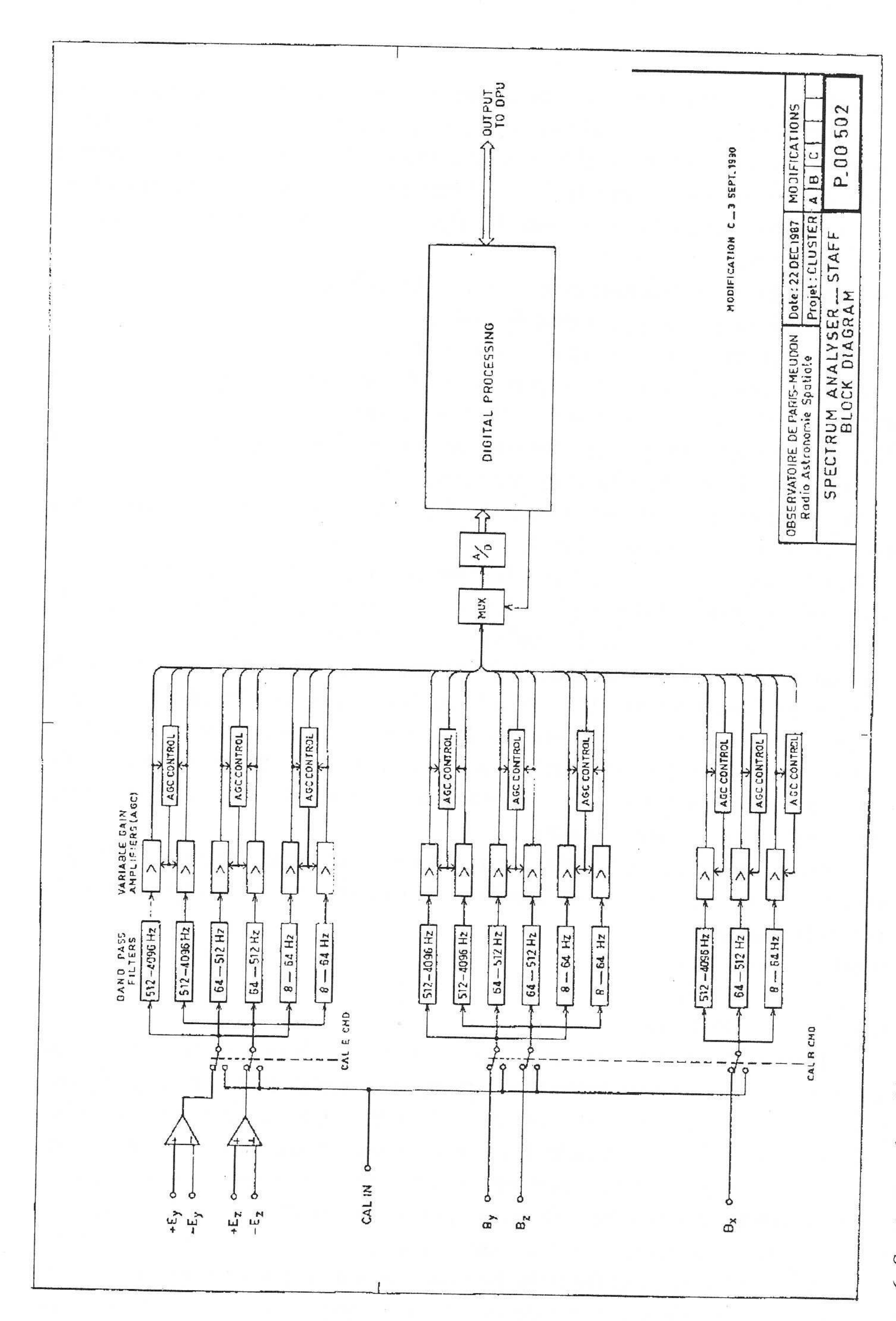
- the magnitude is sampled into one of 8 bins with upper limits distributed approximately as  $2^{-n}$ , for n = 0 to 7;
- the precision of the phase depends upon the magnitude of the coherence: for a signal with magnitude in the highest bin, it is approximately  $5^{\circ}$  close to  $0^{\circ}$ ,  $180^{\circ}$ , and  $\pm 90^{\circ}$ , increasing to about  $10^{\circ}$  midway between these angles.

The spectral estimates are made at 27 frequencies distributed logarithmically over the range from 8 Hz to 4 kHz. All channels are sampled simultaneously, and the integration time for each channel is the same as the overall instrument time resolution, which can be commanded to values between 125 ms (except at the lowest frequencies) and 4 s. The cross-spectra are generally telemetered 4 times less frequently than the auto-spectra.

The frequency range of 8–4000 Hz is divided into three logarithmically distributed frequency sub-bands, each with a maximum frequency eight times the minimum frequency:

Band A: 8–64 Hz, Band B: 64–512 Hz, Band C: 512–4000 Hz.

The 'front end' of the analyser is analogue. For each of the three bands and for each of the five sensors there is a separate automatic gain-controlled (AGC) amplifier and separate band-pass filtering. This pre-conditioning normalises the overall output signal level within each sub-band to an optimum level for digitisation. The subsequent digital filtering performs the fine frequency analysis. The gain of these AGC amplifiers has the role of a multiplying factor in the determination of the absolute measurement. In the case of the spin-plane components (Ey, Ez and By, Bz) the total power from the two sensors is used for the normalisation, to remove the spin modulation. Separate high- and low-pass filters ensure that the gain normalisation is performed only for signal components with frequency within the



3 bandw coefficients, transmitted to th search coil, analogue filtering in spectral matrix get the ser block diagram. From left to right: interface with EFW 2 the spinning components) and the digital processing to Figure 6. Spectrum analyser block diagram. controls (that couple 2 by 2 the spinning con

band which will be further analysed digitally and, more importantly, they prevent 'aliasing' by frequencies above the Nyquist frequency.

The outputs from the 15 amplifiers are multiplexed to a single 8-bit 'flash' analogue/digital converter. They are digitised at a rate of 16 kHz, in a rapid-fire mode by groups of 5 or 10, as needed. The 9 AGC gain-control signals are digitised separately for inclusion in the telemetry.

The digital processing (block at the right hand side of Figure 6) of the sampled inputs is performed in three distinct steps:

- de-spin of the spin-plane sensor outputs;
- determination of the complex Fourier coefficients;
- calculation of the correlation matrices.

The de-spinning operation involves taking the signals from the two pairs of sensors, the electric dipoles and the y and z components of the search coil, and combining them so as to create the inputs which would have been received from non-rotating sensors. This transformation is necessary because the instrument measurement time interval is not short compared with the spacecraft spin period. Each pair of samples  $S_y$  and  $S_z$  are used to calculate

$$S_u = S_y \cos(m) + S_z \sin(m) ,$$
  

$$S_v = S_z \cos(m) - S_y \sin(m) ,$$

where m is the instantaneous angular position of the spacecraft as derived from the on-board Sun Reference Pulse (SRP), and u and v are the fixed coordinates.

These calculations are time-consuming. Therefore in band C the calculations are not performed on each individual data pair, but rather at the level of successive spectral matrices, which are computed every 16 ms, during which time the spacecraft has rotated very little.

The Fourier coefficients are determined using algorithms which are extensions of the Remez exchange algorithm (Rabiner and Gold, 1975). Each of the three analogue receiver bands is analysed using an algorithm very similar to the wavelet transform. The analysis divides the 3-octave band into 9 logarithmically-spaced channels, each with a relative 3 dB bandwidth of 26% of its central frequency. The time required for this analysis depends on the frequency band, ranging from 0.016 to 1 s.

The auto- and cross-spectra are calculated by multiplication of the complex Fourier coefficients and accumulation of the products; the 27 frequency channels yield a total of 135 auto-spectral coefficients and 270 complex cross-spectral coefficients. In Normal mode the measurement cycle is 4 s, during which time the analyser returns the auto-spectral coefficients accumulated during four consecutive intervals of 1 s, and the cross-spectral coefficients averaged over 4 s. During accumulation, any inbalance between the spin-plane analogue receivers gives rise to an apparent coupling between the y and z sensors; this will be corrected during ground data processing.

Internally the coefficients are accumulated as 40-bit integers representing spectral power. Of these 40 bits, 24 are significant for the final auto-spectrum; they represent a dynamic range of  $10 \log_{10}(2^{24}) = 72$  dB. To optimise use of the allocated telemetry and to simplify the interface with the DWP the 24-bit amplitudes N are logarithmically compressed into 8-bit telemetry words using 5 bits for the exponent E and 3 bits for the mantissa M, so that

$$N = 2^{(E-3)}(8+M)$$
.

The overall dynamic range for this data representation is 96 dB, while the average resolution is 0.38 dB. The cross-spectral coefficients  $S_{ij}$  are normalised on-board by division by the associated auto-spectral coefficients  $S_{ii}$  and  $S_{jj}$ , to yield the coherence  $C_{ij}$ ,

$$C_{ij} = S_{ij} / \sqrt{S_{ii}S_{jj}} ,$$

which is always less than unity. The real and imaginary parts of  $C_{ij}$ , including their sign, are each encoded in 4 bits.

The dynamic range of the front-end AGC analogue amplifiers is 75 dB, while the digital processor has a dynamic range of 45–50 dB. For the magnetic field, the dynamic range of the analogue amplifiers has been adjusted so that in the highest band of frequencies their maximum gain corresponds to the sensitivity (noise level) of the magnetic antennas. The digital noise introduced by the spectrum analyser is thus negligible, while the analogue receivers still cover the entire dynamic range of 70 dB of the magnetic antennas. In the lower two frequency bands the dynamic range is offset by factors of respectively 8 and 64, i.e., 9 and 18 dB; the lower end of the range is extended using the dynamic range of the digital analyser. For the electric field the dynamic range of the analogue amplifiers has similarly been adjusted with respect to the sensor noise level, to yield an effective dynamic range better than 70 dB at any frequency.

# 4.4. IN FLIGHT CALIBRATION

Calibration can be commanded by the DWP to calibrate in flight the STAFF experiment (the magnetic wave sensors, the waveform unit and the spectrum analyser), either at normal bit rate or at high bit rate. Two kinds of calibration signals are generated in the magnetic waveform unit: either two simultaneous sine waves at around 7 Hz and 100 Hz, or a pseudo-random noise covering 4 kHz bandwidth. One output attenuator covers a 80 dB dynamic range in steps of 13 dB. An example of dynamic spectrum obtained from one component of the wave form data, up to 12 Hz, during an internal calibration period is shown in Figure 7. In the first part of the calibration, one can see the white noise, whose amplitude decreases after 64 s by steps of 13 dB every 16 s, and increases again before sending sine waves,

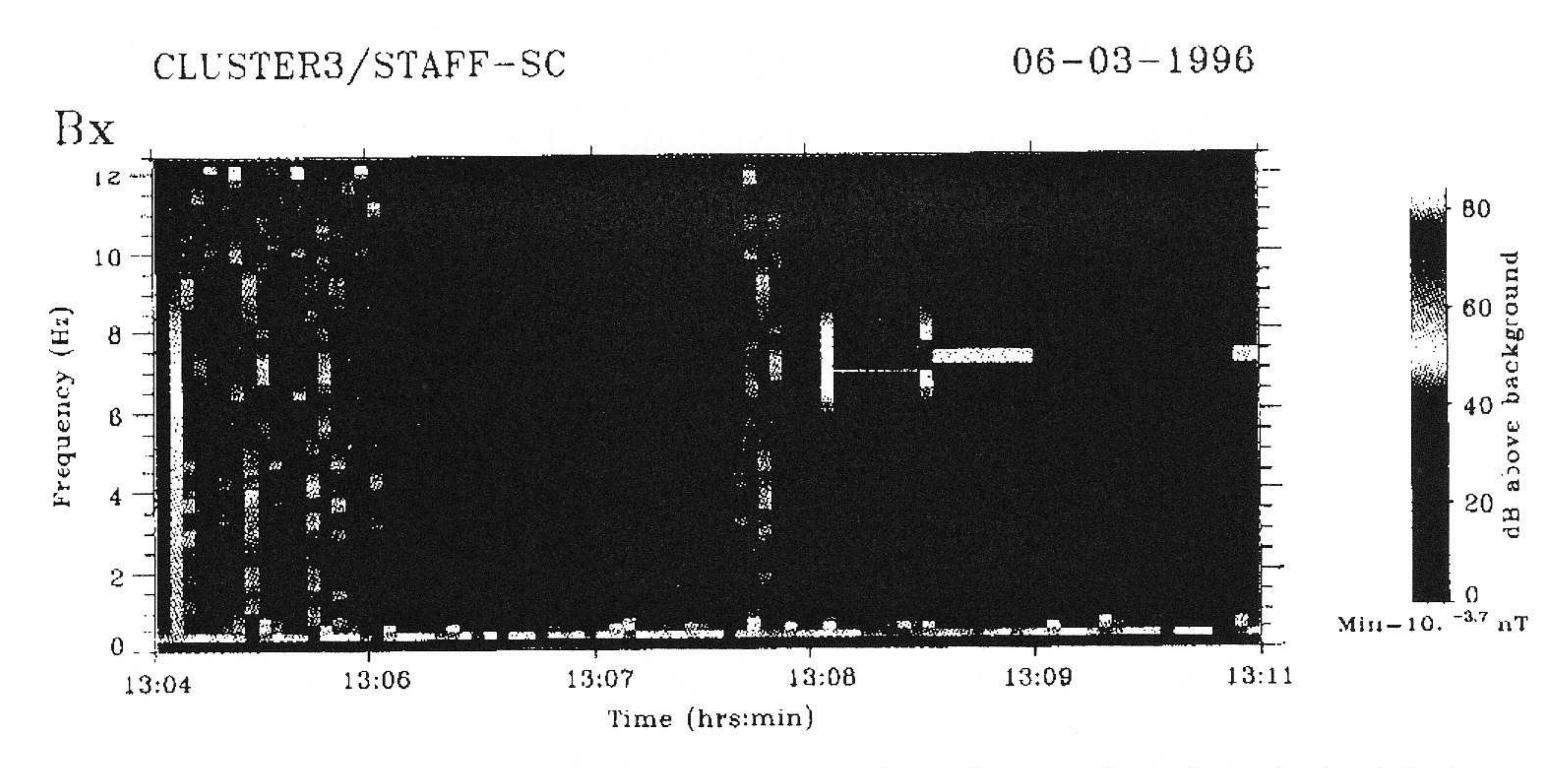


Figure 7. Dynamic spectra of STAFF  $B_x$  component from the waveform data obtained during an internal calibration period in normal bit rate. The calibration comprises 23 steps of 16 s each. In the first part of the calibration, a white noise is generated, whose amplitude decreases after 64 s by steps of 13 dB, and increased again before sending sin waves of about 7 Hz, whose amplitude is also varied by steps of 26 dB.

whose amplitudes are also varied, by steps of 26 dB. In the noisy environment of the ground integrations, the calibration dynamic of 80 dB is achieved, that will be improved in flight conditions. The signal of calibration is transmitted in the telemetry packets, together with the signals coming from the output of the STAFF analysers. It is used as a reference signal for the phase measurements between the different channels. The calibration allows the location of a failure, if any, to be identified in the STAFF chain. The transfer function can be re-established on ground. Special care has been taken with this tool, as it is very important to have accurate calibrations to compare measurements performed at the four spacecraft, as for instance in the calculation of inter-spectra in applying the FED method (see Section 2). The different spectrum analyser modes are also tested during this sequence, allowing to identify possible calculations errors. Modifications of the onboard program can be patched by telecommand, if necessary.

### 4.5. OPERATIONAL MODES

Different operational modes are foreseen, mainly depending on the bit rate. A short description of these modes, for both the waveform and the spectrum analyser is given below (for details, see Tables II–IV). The STAFF modes are part of the WEC modes that are monitored by DWP (Pedersen *et al.*, this issue). Those WEC modes have been defined in order to get the best scientific return. The different constraints, telemetry, Whisper active, Langmuir mode of EFW, and available power have been

Table II
STAFF waveform data modes (search coil)

Mode	Bit rate	Compression	bit s <sup>-1</sup>	
NM	Normal	Yes (12 bits)	928	_
BM	High bit rate	Yes (12 bits)	16 480	
EM NBR	Normal	No (16 bits)	1216	
EM HBR	High bit rate	No (16 bits)	21 760	

Table III
STAFF spectrum analyzer normal bite rate operation modes

Band	Auto	Auto		Cross		AGC	
	resolution	bit s <sup>-1</sup>	resolution	bit s <sup>-1</sup>	resolution	bit s <sup>-1</sup>	
Normal mode 1: NI	$M1 (3 \times B + 2)$	× E) 16	96 bit s <sup>-1</sup> (incl	uding status)			
A: 8–64 Hz	1 s	360	4 s	180	1 s	24	
B: 64-512 Hz	1 s	360	4 s	180	1 s	24	
C: 512–4096 Hz	1 s	360	4 s	180	1 s	24	
Normal modes 1': N	$VM1'b (3 \times B)$	or NM1'e (	$(2 \times E + B_x)$	864 bit s <sup>-1</sup>	(including sta	atus)	
A: 8–64 Hz	1 s	216	4 s	54	1 s	16	
B: 64-512 Hz	1 s	216	4 s	54	1 s	16	
C: 512–4096 Hz	1 s	216	4 s	54	1 s	16	
Normal modes 2: N	$M2b (3 \times B) c$	or NM2e (2	$\times E + B_x$ )	1840 bit s <sup>-1</sup>	(including stat	rus)	
A: 8–64 Hz	1 s	216	1 s	216	1 s 16		
B: 64-512 Hz	0.5 s	432	1 s	216	0.5 s	32	
C: 512-4096 Hz	0.5 s	432	1 s	216	0.5 s	32	
Special mode: SM (	$(3 \times B + 2 \times I)$	E) 3032 b	it s <sup>-1</sup> (includin	ig status)			
A: 8–64 Hz	1 s	360	2 s	360	1 s	24	
B: 64-512 Hz	0.5 s	720	2 s	360	0.5 s	48	
C: 512-4096 Hz	0.5 s	720	2 s	360	0.5 s	48	
Emergency mode: E	$EM(3 \times B + 2)$	$\times E$ ) 11.	$20 \text{ bit s}^{-1} \text{ (incl}$	uding status)			
A: 8–64 Hz	2 s	180	4 s	180	2 s	12	
B: 64-512 Hz	2 s	180	4 s	180	2 s	12	
C: 512-4096 Hz	2 s	180	4 s	180	2 s	12	

considered in the choice of the modes (Pedersen et al., this issue). The WEC modes can be modified if necessary.

The principle is to cover the full STAFF frequency range in all modes, but the methods are different depending on the bit rate. In normal bit rate, the waveform data covers the 0.1–10 Hz frequency range, whereas the spectrum analyser covers

Table IV
STAFF spectrum analyser high bit rate operation modes

Band	Auto		Cross		AGC	
	resolution	bit s <sup>-1</sup>	resolution	bit s <sup>-1</sup>	resolution	bit s <sup>-1</sup>
Fast mode 1: FM1 (3	$\times$ $B$ + 2 $\times$	E) 7600	bit s <sup>-1</sup> (inclu	ding status)		
B: 64-512 Hz	0.125 s	2880	1 s	720	0.125 s	192
C: 512-4096 Hz	0.125 s	2880	1 s	720	0.125 s	192
Fast mode 2: FM2 (3	$\times$ $B$ + 2 $\times$	E) 4528	bit $s^{-1}$ (inclu	ding status)		
B: 64-512 Hz	0.25 s	1440	1 s	720	0.25 s	96
C: 512-4096 Hz	0.25 s	1440	1 s	720	0.25 s	96
Fast mode 3: FM3b (	$(3 \times B)$ or F	M3e ( $2 \times E$	$+ B_x$ ) 41	$60 \text{ bit s}^{-1}$ (in	ncluding stati	as)
B: 64-512 Hz	0.125 s	1728	1 s	216	0.125 s	128
C: 512-4096 Hz	0.125 s	1728	1 s	216	0.125 s	128

the frequency range 8 Hz–4 kHz, working in its three frequency bands. In high bit rate (also called burst mode), the waveform data covers the 0.1–180 Hz frequency range, and in order to save telemetry, the spectrum analyser only operates in its two upper frequency bands, from 64 Hz to 4 kHz.

For the waveform data, two combinations of commands can be sent, one is the sampling frequency rate, the other is whether a data compression is applied or not (see Section 4.2). In normal bit rate, the sampling frequency is 25 Hz, associated with the 10 Hz low pass filter. In high bit rate, the sampling frequency is 450 Hz, with the 180 Hz filter. STAFF and EFW use the same sampling frequency, synchronised by DWP. Thus there are four STAFF waveform data modes (see Table II). The NM mode, in normal telemetry rate with compression, giving a bit rate of 928 bit s<sup>-1</sup>. In emergency mode the 16-bit words are telemetered (EM NBR mode). The principle is the same in high bit rate; with data compression, the needed telemetry is 16 480 bit s<sup>-1</sup> (BM mode).

For the spectrum analyser, the different modes have been defined by combining three parameters: the time resolution, the number of frequencies computed and the number of wave components considered. The modes are defined to fulfil different scientific objectives, in the framework of three constraints, first the telemetry limitation, second the total WEC power limitation, then the operations mode of the other WEC experiments, as discussed in Pedersen *et al.* (this issue).

Normal Mode 1 (NM1) is the basic mode in normal bit rate. The auto-spectra are averaged over 1s, and the complete matrix over 4s for five components (25 coefficients). The other modes are variations of this.

In Normal Mode 1' (NM1'), the calculation is performed for only three components, either  $3 \times \mathbf{B}$  (NM1'b) or  $B_x$  plus  $2 \times E$  (NM1'e). Only nine elements of the spectral matrix are computed (out of 25). This mode is used in time-sharing with NM1, during periods when Whisper is active.

In Normal Mode 2 (NM2), three of the five wave components are selected as in NM1'. The time resolution is 0.5 or 1 s for the auto-spectra and 1 s for the cross-spectra. This mode is a 'low power' mode, and the input of the components that are not used are powered off. When the modes NM2b and NM2e are used in time-sharing, the AGC needs some time to recover. The mode NM2b can also be used when EFW is in Langmuir mode and not in electric field measurement mode on all four booms, as the calculation of the de-spun electric components needs the two spinning components.

In Special Mode the time resolution is improved. This mode can be used if for some reason, more telemetry is available to STAFF inside WEC in normal bit rate.

In Emergency Mode, the five components are used, with a lower time resolution of 2 and 4 s for the auto- and cross-spectra, respectively. This reduction in time resolution, and thus in telemetry is intended to compensate for the telemetry increase due to the non-compression of the waveform data, in case DWP cannot perform the waveform compression.

In high bit rate (also called burst mode), the spectral matrix coefficients are calculated only in the two highest frequency bands. In the Fast Modes the time resolution is 1 s for the cross-spectra and either 0.125 s or 0.25 s for the auto-spectra. Here again five or three components can be considered (see Table IV).

The calibration mode calibrates both parts of the experiment, the magnetic wave form and the spectrum analyser (see Section 4.4). It is foreseen to operate the calibration program no more than once a day, or rather once per orbit, and preferably at the beginning of a data acquisition sequence. The duration of the calibration sequence is about 6 min at normal bit rate and 2 min in burst mode.

# 4.6. GSE AND INTEGRATION SOFTWARE

Specific STAFF software to test the instrument capabilities has been written by the STAFF team (Table I), whereas the overall WEC testing is under responsibility of DWP (Pedersen *et al.*, this issue). The decommutation of the WEC packets into STAFF data packets is done by DWP, as for other WEC instruments. The GSE software has been used as the starting point of the ground segment software. The ground software includes the instrument monitoring, the preparation of STAFF parameters for the Cluster Science Data System (CSDS) (Schmidt and Escoubet, this issue), and of course scientific data analysis. The role of DWP in this facilitates the use of a common software to analyse simultaneously data coming from different WEC instruments. The definition and the implementation of this common software are coordinated by the WEC Data Working Group (Pedersen *et al.*, this issue).

#### 5. Conclusion

The STAFF experiment consists of a set of four state-of-the-art instruments to measure and analyse the vector magnetic field fluctuations and, in the appropri-

ate frequency range, correlate them with the two components of the electric field measured by the EFW experiment. STAFF will thus optimise the global Cluster scientific return, particularly in those regions of space that are primary scientific targets for the mission. The instruments on each individual spacecraft will produce significant new data and, furthermore, the four instruments are identical, and have sufficient resolution, to allow good separation of spatial and temporal variations of the measured parameters. The experiment is well characterised by its calibration model; the parameters of this model will be checked regularly and updated if necessary, using data acquired during the calibration cycle which is executed routinely throughout the mission.

Thus STAFF will make accurate estimates of important wave properties in the frame of reference of each spacecraft. Using data from the four instruments, alone or in combination with other WEC data such as the EFW convection (DC) and waveform data, it will generally be possible to determine wave properties in the physically more important rest frame of the plasma. Comparison with simultaneous particle measurements will be essential to study the physical processes. To this end, STAFF is participating actively in the implementation of the Cluster Science Data System, which is the essential first step towards the coordinated studies of high-resolution data.

### Acknowledgements

The realisation, testing, integration of the STAFF experiment, as well as the preparation of the ground software for instrument commanding, health verification and science analysis have benefited of the help of many people, in many places. We would like to thank: M. Belkacemi, D. Carrière, A. C. Gueriau, J. P. Mengué, A. Rapin, J. P. Rivet, L. Sitruk (DESPA/Meudon Observatory), D. Bagot, V. Bouzid, N. Denis, E. François, A. Mayaki (CETP), A. Butler, D. Klinge (SSD/ESTEC). The WEC, ESA, and Dornier teams are thanked for the co-operative help in the design, testing and integration of the experiment. H. Poussin, M. Nonon, J. Y. Prado, and J. P. Thouvenin at CNES are thanked for their continuous assistance and co-operation in the STAFF CSDS data handling preparation, as are the JSOC and ESOC teams in the preparation of the operations. The STAFF experiment and software are realised thanks to CNES support, through contract with CETP, DESPA, and LPCE. The University of Versailles Saint-Quentin is thanked for its support to CETP Cluster team. The referees are thanked for their fruitful comments.

# References

Anderson, B. J., Fuselier, S. A., and Murr, D.: 1991, 'Electromagnetic Ion Cyclotron Waves Observed in the Plasma Depletion Layer', *Geophys. Res. Letters* 18, 1955-1958.

Anderson, B. J., Fuselier, S. A., Gary, S. P., and Denton, R. E.: 1994, 'Magnetic Spectral Signatures in the Earth's Magnetosheath and Plasma Depletion Layer', *J. Geophys. Res.*. **99**, 5877.

- Belkacemi, M.: 1994, 'Modélisation et Qualification de l'Analyseur Multicanal Numérique Temps Réel à Corrélation STAFF SA pour l'Expérience Spatiale Européenne Cluster', PhD Thesis, Paris 6 University.
- Belkacemi, M., Bougeret, J.-L., Cornilleau-Wehrlin, N., Friel, L, Harvey, C. C., Manning, R., and Parrot, M.: 1993, 'Determination Characteristics of the STAFF Spectrum Analyser using Simulated Data', *Proc. of ESA conference on Spatio-Temporal Analysis for Resolving Plasma Turbulence*, Aussois, France, 31 January–5 February, 1993, ESA WPP-047.
- Belmont, G., Reberac, F., and Rezeau, L.: 1995, 'Resonant Amplification of Magnetosheath MHD Fluctuations at the Magnetopaus'e, *Geophys. Res. Letters* 22, 295.
- Blanco-Cano, X. and Schwartz, S. J.: 1996, 'AMPTE-UKS Observations of ULF Waves in the Quasi-Parallel Ion Foreshock', *J. Geophys. Res.*, in press.
- Büchner, J. M. and Zelenyi, L. M.: 1988, Adiabatic Chaotic and Quasi-adiabatic Charged Particle Motion in Two-dimensional Magnetic Field Reversals, ESA SP-285, 1, 219.
- Burgess, D.: 1995, 'Foreshock-Shock Interaction at Collisionless Quasi-parallel Shocks', Adv. Space Res. 15 (8/9), 159.
- Cattell, C., Wygant, J., Mozer, F. S., Okada, T., Tsuruda, K., Kokubun, S., and Yamamoto, T.: 1995, 'ISEE 1 and Geotail observations of Low-Frequency Waves at the Magnetopause', *J. Geophys. Res.* **100**, 11823.
- Delcourt, D. C., Martin, R. F., Jr., Sauvaud, J.-A., and Moore, T. E.: 1995, 'The Centrifugal Trapping in the Magnetotail', *Ann. Geophys.* 13, 242.
- Dubouloz, N. and Scholer, M.: 1995, 'Two-Dimensional Simulations of Magnetic Pulsations Upstream of the Earth's Bow Shock', *J. Geophys. Res.* 100, 9461.
- Fredericks, R. W., Scarf, F. L., and Russell, C. T.: 1973, 'Field-Aligned Currents, Plasma Waves, and Anomalous Resistivity in the Disturbed Polar Cap', J. Geophys. Res. 78, 2133.
- Fuselier, S. A.: 1995, 'Ion Distributions in the Earth's Foreshock Upstream from the Bow Shock', Adv. Space Res. 15 (8/9), 43.
- Gendrin, R.: 1983, 'Magnetic Turbulence and Diffusion Processes in the Magnetopause Boundary Layer', Geophys. Res. Letters 10, 769.
- Greenstadt, E. W., Le, G., and Strangeway, R. J.: 1995, 'ULF Waves in the Foreshock', Adv. Space Res. 15 (8/9), 71.
- Gurnett, D. A.: 1985, in B. T. Tsurutani and R. G. Stone (eds.), 'Plasma Waves Instabilities, Collisionnless Shocks in the Heliosphere: Reviews of Current Research', *Geophys. Monogr. Ser.*, Vol. 35, AGU, Washington, D.C., p. 207.
- Gustafsson, G. et al.: 1996, this issue.
- Haerendel, G., Paschman, G., Sckopke, N., Rosenbauer, H., and Hedgecock, P. C.: 1978, 'The Frontside Boundary Layer of the Magnetosphere and the Problem of Reconnection', *J. Geophys. Res.* 83, 3195.
- Hellinger, P., Mangeney, A., and Matthews, A.: 1995, 'Whistler Waves in 3D Hybrid Simulations of Quasi-Perpendicular Shocks', *Geophys. Res. Letters* 22, 2091.
- Hubert, D.: 1994, 'Nature and Origin of Wave Modes in the Dayside Earth Magnetosheath', Adv. Space Res. 14 (7), 55.
- Krauss-Varban, D.: 1994, 'Bow Shock and Magnetosheath Simulations: Wave Transport and Kinetic Properties, Solar Wind Sources of Magnetospheric Ultra-Low-Frequency Waves', *Geophysical Monograph* 81, 121.
- Krauss-Varban, D., Pantellini, F. E. G., and Burgess, D.: 1995, 'Electron Dynamics and Whistler Waves at Quasi-Perpendicular Shocks', *Geophys. Res. Letters*, in press.
- Khurana, K. K., Kivelson, M. G., Frank, L. A., and Paterson, W. R.: 1995, 'Observations of Magnetic Flux Ropes and Associated Currents in Earth's Magnetotail with the Galileo Spacecraft', *Geophys. Res. Letters* 22, 2087.
- Labelle, J. and Treumann, R. A.: 1988, 'Plasma Waves at the Dayside Magnetopause', Space Sci. Rev. 47, 175.
- Lacombe, C. and Belmont, G.: 1995, 'Waves in the Earth's Magnetosheath: Observations and Interpretations', Adv. Space Res. 15 (8/9), 329.
- Le, G., Russell, C. T., Thomsen, M. F., and Gosling, J. T.: 1992, 'Observations of a New Class of Upstream Waves with Periods near 3 Seconds', J. Geophys. Res. 97, 2917.

- Le, G., Russell, C. T., and Orlowski, D. S.: 1993, 'Coherence Length of Upstream ULF Waves: Dual ISEE Observations', *Geophys. Res. Letters* 20, 1755.
- Lefeuvre, F., Parrot, M., and Delannoy, C.: 1981, 'Wave Distribution Functions Estimation of VLF Electromagnetic Waves Observed On-Board GEOS-1', J. Geophys. Res. 86, 2359.
- Louarn, P., Roux, A., de Féraudy, H., and LeQuéau, D.: 1990, 'Trapped Electrons as a Free Energy Source for the Auroral Kilometric Radiation', *J. Geophys. Res.* **95**, 5983.
- Louarn, P., Wahlung, J. E., Chust, T., de Feraudy, H., Roux, A., Holback, B., Dovner, P. O., Eriksson, A., and Holmgren, G.: 1994, 'Observation of Kinetic Alfvén Waves by the Freja Spacecraft', *J. Geophys. Res.* **99**, 23 623.
- Lui, A. T. Y., Lopez, R. E., Anderson, B. J., Takahashi, K., Zanetti, L. J., McEntire, R. W., Potemra, T. A., Klumpar, D. M., Greene, E. M., and Strangeway, R.: 1992, 'Current Disruption in the Near-Earth Neutral Sheet Region', *J. Geophys. Res.* 97 1461.
- Matsumoto, H., Kojima, H., Miyatake, T., Omura, Y., Okada, M., Nagano, I., and Tsutsui, M.: 1994, 'Electrostatic Solitary Waves (ESW) in the Magnetotail: BEN Waveforms Observed by Geotail', *Geophys. Res. Letters* 25, 2915.
- McPherron, R. L., Russel, C. T., and Coleman, J. R., Jr.: 1972, 'Fluctuating Magnetic Waves in the Magnetosphere, 2, ULF Waves', *Space Sci. Rev.* 13, 411.
- Means, J. D.: 1972, 'Use of the Three-Dimensional Covariance Matrix in Analysing the Polarisation Properties of Plane Waves', *J. Geophys. Res.* 77, 5551.
- Mitchell, D. G., Williams, D. J., Huang, C. Y., Frank, L. A., and Russel, C. T.: 1990, 'Current Carriers in the Near-Earth Cross-Tail Current Sheet During Substorm Growth Phase', *Geophys. Res. Letters* 17, 3131.
- Paschman, G. et al.: 1996, this issue.
- Pedersen, A. et al.: 1996, this issue.
- Perraut, S., Morane, A., Roux, A., Pedersen, A., Schmidt, R., Korth, A., Kremser, G., Apariciao, B., and Pellinen, R. J.: 1993, 'Characterisation of Small Scale Turbulence Observed at Substorm Onset: Relationships with Parallel Acceleration of Particles', *Adv. Space. Res.* 13, 217.
- Perraut, S., Roux, A., Holter, O., Korth, A., Kremser, G., and Pedersen, A.: 1995, Current Sheet Structure and Relation to Breakup, ESA SP-371, p. 239.
- Phan, T.-D., Paschmann, G., Baumjohann, W., Sckopke, N., and Lühr, H.: 1994, 'The Magnetosheath Region Adjacent to the Dayside Magnetopause: AMPTE/IRM Observations', *J. Geophys. Res.* 99, 121.
- Pinçon, J. L. and Lefeuvre, F.: 1991, 'Local Characterization of Homogeneous Turbulence in a Space Plasma from Simultaneous Measurements of Field Components at Several Points in Space', J. Geophys. Res. 96, 1789.
- Pinçon, J. L. and Lefeuvre, F.: 1992, 'The Application of the Generalized Capon Method to the Analysis of a Turbulent Field in Space Plasma: Experimental Constraints', *J. Atmospheric Terrest. Phys.* **54**, 1237.
- Pinçon, J. L., Lefeuvre, F., and Parrot, M.: 1990, 'Experimental Constraints in the Characterisation of a Turbulent Field from Several Satellites', *Proc. Int. Workshop on Space Plasma Physics Investigations by Cluster and Regatta*, Graz, ESA SP-306, p. 57.
- Rabiner and Gold: 1975, Theory and Application of Digital Signal Processing, Prentice-Hall, New York.
- Rezeau, L., Morane, A., Perraut, S., Roux, A., and Schmidt, R.: 1989, 'Characterization of Alfvénic Fluctuations in the Magnetopause Boundary Layer', *J. Geophys. Res.* 94, 101.
- Rezeau, L., Roux, a., and Cornilleau-Wehrlin, N.: 1990, 'Multipoint Study of Small Scale Structures at the Magnetopause', *Proc. Int. Workshop on Space Plasma Physics Investigations by Cluster and Regatta*, Graz, February 1990, ESA SP-306, p. 103.
- Rezeau, L., Roux, A., and Russell, C. T.: 1993, 'Characterization of Small Scale Structures at the Magnetopause from ISEE Measurements', *J. Geophys. Res.* 98, 179.
- Robert, P., Gendrin, R., Perraut, S., Roux, A., and Pedersen, A.: 1984, 'GEOS-2 Identification of Rapidly Moving Current Structures in the Equatorial Outer Magnetosphere During Substorms', J. Geophys. Res. 89, 819.
- Russell, C. T., Childers, D. D., and Coleman, P. J., Jr.: 1971, 'OGO-5 Observations of Upstream Waves in the Interplanetary Medium: Discrete Wave Packets', *J. Geophys. Res.* 76, 845.

- Santolik, O.: 1993, 'Etude sur les Directions Normales des Ondes Electromagnétiques dans un Plasma', LPCE/NTS/018.A.
- Savoini, P. and Lembège, B.: 1994, 'Electron Dynamics in Two and One Dimensional Oblique Supercritical Collisionless Magnetosonic Shocks', *J. Geophys. Res.* 99, 6609.
- Savoini, P. and Lembège, B.: 1995, 'Heating and Acceleration of Electrons through the Whistler Precursor in 1D and 2D Oblique Shocks', *Adv. Space Res.* **15** (8/9), 235.
- Schmidt, R. and Escoubet, C. P.: 1996, 'The Cluster Science Data System', this issue.
- Scholer, M.: 1995, 'Interaction of Upstream Diffuse Ions with the Solar Wind', Adv. Space Res. 15 (8/9), 125.
- Scudder, J. D., Mangeney, A., Lacombe, C., Harvey, C. C., Wu, C. S., and Anderson, R. R.: 1986, 'The Resolved Layer of a Collisionless, High b, Supercritical, Quasi-perpendicular Shock Wave: 3. Vlasov Electrodynamics', *J. Geophys. Res.* **91**, 11 074.
- Sentman, D. D., Thomsen, M. F., Gary, S. P., Feldman, W. C., and Hoppe, M. M.: 1983, 'The Oblique Whistler Instability in the Earth's Foreshock', *J. Geophys. Res.* 88, 2048.
- Song, P.: 1994, 'ISEE Observations of the Dayside Magnetosheath', Adv. Space Res. 14, 71.
- Temerin, M. and Lysal, R. L.: 1984, 'Electromagnetic Ion Cyclotron Mode (ELF) Waves Generated by Auroral Electron Precipitation', *J. Geophys. Res.* 89, 2849.
- Vautard, R., Yiou, P., and Ghil, M.: 1992, 'Singular-Spectrul Analysis, A Toolkit for Short, Noisy Chaotic Signals', *Physica* **D58**, 95.
- Veltri, P., Mangeney, A., and Scudder, J. D.: 1990, 'Electron Heating in Quasi-Perpendicular Shocks: a Monte Carlo Simulation', *J. Geophys. Res.* **95**, 14939.
- Wahlund, J. E., Louarn, P., Chust, T., de Feraudy, H., Roux, A., Holback, B., Cabrit, B., Eriksson, A. I., Kintner, P. M., Kelley, M. C., Bonnel, J., and Chesney, S.: 1994, 'Observations of Ion Acoustic Fluctuations in the Auroral Topside Ionosphere by Freja S/C', *Geophys. Res. Letters* 21, 1835.
- Winske, D., Omidi, N., Quest, K. B., and Thomas, V. A.: 1990, 'Reforming Supercritical Quasi-Parallel Shocks, 2., Mechanisms for Wave Generation and Front Re-formation', *J. Geophys. Res.* **95**, 18821.
- Woolliscroft, L. J. C. et al.: 1996, this issue.
- Youssef, A., Meyer, A., Ducrocq, J. B., and Roux, A.: 1991, 'New Technologies for Integrating Thermal Control and Radiation Protection in Hybrid Technology', *Proc. ESA Electronic Components Conference*, ESTEC, Noordwijk, ESA SP-313.
- Zhang, T.-L., Schwingenschuh, K., and Russell, C. T.: 1995, 'A Study of the Solar Wind Deceleration in the Earth's Foreshock Region', *Adv. Space Res.* **15** (8/9), 137.